BABAR-PUB-03/027
SLAC-PUB-10141

Measurements of the Branching Fractions of Charged B Decays to $K^{\pm}\pi^{\mp}\pi^{\pm}$ Final States

B. Aubert,[1] R. Barate,[1] D. Boutigny,[1] J.-M. Gaillard,[1] A. Hicheur,[1] Y. Karyotakis,[1] J. P. Lees,[1] P. Robbe,[1] V. Tisserand,[1] A. Zghiche,[1] A. Palano,[2] A. Pompili,[2] J. C. Chen,[3] N. D. Qi,[3] G. Rong,[3] P. Wang,[3] Y. S. Zhu,[3] G. Eigen,[4] I. Ofte,[4] B. Stugu,[4] G. S. Abrams,[5] A. W. Borgland,[5] A. B. Breon,[5] D. N. Brown,[5] J. Button-Shafer,[5] R. N. Cahn,[5] E. Charles,[5] C. T. Day,[5] M. S. Gill,[5] A. V. Gritsan,[5] Y. Groysman,[5] R. G. Jacobsen,[5] R. W. Kadel,[5] J. Kadyk,[5] L. T. Kerth,[5] Yu. G. Kolomensky,[5] J. F. Kral,[5] G. Kukartsev,[5] C. LeClerc,[5] M. E. Levi,[5] G. Lynch,[5] L. M. Mir,[5] P. J. Oddone,[5] T. J. Orimoto,[5] M. Pripstein,[5] N. A. Roe,[5] A. Romosan,[5] M. T. Ronan,[5] V. G. Shelkov,[5] A. V. Telnov,[5] W. A. Wenzel,[5] K. Ford,[6] T. J. Harrison,[6] C. M. Hawkes,[6] D. J. Knowles,[6] S. E. Morgan,[6] R. C. Penny,[6] A. T. Watson,[6] N. K. Watson,[6] K. Goetzen,[7] T. Held,[7] H. Koch,[7] B. Lewandowski,[7] M. Pelizaeus,[7] K. Peters,[7] H. Schmuecker,[7] M. Steinke,[7] N. R. Barlow,[8] J. T. Boyd,[8] N. Chevalier,[8] W. N. Cottingham,[8] M. P. Kelly,[8] T. E. Latham,[8] C. Mackay,[8] F. F. Wilson,[8] K. Abe,[9] T. Cuhadar-Donszelmann,[9] C. Hearty,[9] T. S. Mattison,[9] J. A. McKenna,[9] D. Thiessen,[9] P. Kyberd,[10] A. K. McKemey,[10] V. E. Blinov,[11] A. D. Bukin,[11] V. B. Golubev,[11] V. N. Ivanchenko,[11] E. A. Kravchenko,[11] A. P. Onuchin,[11] S. I. Serednyakov,[11] Yu. I. Skovpen,[11] E. P. Solodov,[11] A. N. Yushkov,[11] D. Best,[12] M. Bruinsma,[12] M. Chao,[12] D. Kirkby,[12] A. J. Lankford,[12] M. Mandelkern,[12] R. K. Mommsen,[12] W. Roethel,[12] D. P. Stoker,[12] C. Buchanan,[13] B. L. Hartfiel,[13] B. C. Shen,[14] D. del Re,[15] H. K. Hadavand,[15] E. J. Hill,[15] D. B. MacFarlane,[15] H. P. Paar,[15] Sh. Rahatlou,[15] V. Sharma,[15] J. W. Berryhill,[16] C. Campagnari,[16] B. Dahmes,[16] N. Kuznetsova,[16] S. L. Levy,[16] O. Long,[16] A. Lu,[16] M. A. Mazur,[16] J. D. Richman,[16] W. Verkerke,[16] T. W. Beck,[17] J. Beringer,[17] A. M. Eisner,[17] C. A. Heusch,[17] W. S. Lockman,[17] T. Schalk,[17] R. E. Schmitz,[17] B. A. Schumm,[17] A. Seiden,[17] M. Turri,[17] W. Walkowiak,[17] D. C. Williams,[17] M. G. Wilson,[17] J. Albert,[18] E. Chen,[18] G. P. Dubois-Felsmann,[18] A. Dvoretskii,[18] D. G. Hitlin,[18] I. Narsky,[18] F. C. Porter,[18] A. Ryd,[18] A. Samuel,[18] S. Yang,[18] S. Jayatilleke,[19] G. Mancinelli,[19] B. T. Meadows,[19] M. D. Sokoloff,[19] T. Abe,[20] F. Blanc,[20] P. Bloom,[20] S. Chen,[20] P. J. Clark,[20] W. T. Ford,[20] U. Nauenberg,[20] A. Olivas,[20] P. Rankin,[20] J. Roy,[20] J. G. Smith,[20] W. C. van Hoek,[20] L. Zhang,[20] J. L. Harton,[21] T. Hu,[21] A. Soffer,[21] W. H. Toki,[21] R. J. Wilson,[21] J. Zhang,[21] D. Altenburg,[22] T. Brandt,[22] J. Brose,[22] T. Colberg,[22] M. Dickopp,[22] R. S. Dubitzky,[22] A. Hauke,[22] H. M. Lacker,[22] E. Maly,[22] R. Müller-Pfefferkorn,[22] R. Nogowski,[22] S. Otto,[22] J. Schubert,[22] K. R. Schubert,[22] R. Schwierz,[22] B. Spaan,[22] L. Wilden,[22] D. Bernard,[23] G. R. Bonneaud,[23] F. Brochard,[23] J. Cohen-Tanugi,[23] P. Grenier,[23] Ch. Thiebaux,[23] G. Vasileiadis,[23] M. Verderi,[23] A. Khan,[24] D. Lavin,[24] F. Muheim,[24] S. Playfer,[24] J. E. Swain,[24] M. Andreotti,[25] V. Azzolini,[25] D. Bettoni,[25] C. Bozzi,[25] R. Calabrese,[25] G. Cibinetto,[25] E. Luppi,[25] M. Negrini,[25] L. Piemontese,[25] A. Sarti,[25] E. Treadwell,[26] F. Anulli,[27,*] R. Baldini-Ferroli,[27] M. Biasini,[27,*] A. Calcaterra,[27] R. de Sangro,[27] D. Falciai,[27] G. Finocchiaro,[27] P. Patteri,[27] I. M. Peruzzi,[27,*] M. Piccolo,[27] M. Pioppi,[27,*] A. Zallo,[27] A. Buzzo,[28] R. Capra,[28] R. Contri,[28] G. Crosetti,[28] M. Lo Vetere,[28] M. Macri,[28] M. R. Monge,[28] S. Passaggio,[28] C. Patrignani,[28] E. Robutti,[28] A. Santroni,[28] S. Tosi,[28] S. Bailey,[29] M. Morii,[29] E. Won,[29] W. Bhimji,[30] D. A. Bowerman,[30] P. D. Dauncey,[30] U. Egede,[30] I. Eschrich,[30] J. R. Gaillard,[30] G. W. Morton,[30] J. A. Nash,[30] P. Sanders,[30] G. P. Taylor,[30] G. J. Grenier,[31] S.-J. Lee,[31] U. Mallik,[31] J. Cochran,[32] H. B. Crawley,[32] J. Lamsa,[32] W. T. Meyer,[32] S. Prell,[32] E. I. Rosenberg,[32] J. Yi,[32] M. Davier,[33] G. Grosdidier,[33] A. Höcker,[33] S. Laplace,[33] F. Le Diberder,[33] V. Lepeltier,[33] A. M. Lutz,[33] T. C. Petersen,[33] S. Plaszczynski,[33] M. H. Schune,[33] L. Tantot,[33] G. Wormser,[33] V. Brigljević,[34] C. H. Cheng,[34] D. J. Lange,[34] D. M. Wright,[34] A. J. Bevan,[35] J. P. Coleman,[35] J. R. Fry,[35] E. Gabathuler,[35] R. Gamet,[35] M. Kay,[35] R. J. Parry,[35] D. J. Payne,[35] R. J. Sloane,[35] C. Touramanis,[35] J. J. Back,[36] P. F. Harrison,[36] H. W. Shorthouse,[36] P. Strother,[36] P. B. Vidal,[36] C. L. Brown,[37] G. Cowan,[37] R. L. Flack,[37] H. U. Flaecher,[37] S. George,[37] M. G. Green,[37] A. Kurup,[37] C. E. Marker,[37] T. R. McMahon,[37] S. Ricciardi,[37] F. Salvatore,[37] G. Vaitsas,[37] M. A. Winter,[37] D. Brown,[38] C. L. Davis,[38] J. Allison,[39] R. J. Barlow,[39] A. C. Forti,[39] P. A. Hart,[39] M. C. Hodgkinson,[39] F. Jackson,[39] G. D. Lafferty,[39] A. J. Lyon,[39] J. H. Weatherall,[39] J. C. Williams,[39] A. Farbin,[40] A. Jawahery,[40] D. Kovalskyi,[40] C. K. Lae,[40] V. Lillard,[40] D. A. Roberts,[40] G. Blaylock,[41] C. Dallapiccola,[41] K. T. Flood,[41] S. S. Hertzbach,[41] R. Kofler,[41] V. B. Koptchev,[41] T. B. Moore,[41] S. Saremi,[41] H. Staengle,[41] S. Willocq,[41] R. Cowan,[42] G. Sciolla,[42] F. Taylor,[42] R. K. Yamamoto,[42] D. J. J. Mangeol,[43] P. M. Patel,[43]

A. Lazzaro,[44] F. Palombo,[44] J. M. Bauer,[45] L. Cremaldi,[45] V. Eschenburg,[45] R. Godang,[45] R. Kroeger,[45] J. Reidy,[45] D. A. Sanders,[45] D. J. Summers,[45] H. W. Zhao,[45] S. Brunet,[46] D. Cote-Ahern,[46] C. Hast,[46] P. Taras,[46] H. Nicholson,[47] C. Cartaro,[48] N. Cavallo,[48, †] G. De Nardo,[48] F. Fabozzi,[48, †] C. Gatto,[48] L. Lista,[48] P. Paolucci,[48] D. Piccolo,[48] C. Sciacca,[48] M. A. Baak,[49] G. Raven,[49] J. M. LoSecco,[50] T. A. Gabriel,[51] B. Brau,[52] K. K. Gan,[52] K. Honscheid,[52] D. Hufnagel,[52] H. Kagan,[52] R. Kass,[52] T. Pulliam,[52] Q. K. Wong,[52] J. Brau,[53] R. Frey,[53] C. T. Potter,[53] N. B. Sinev,[53] D. Strom,[53] E. Torrence,[53] F. Colecchia,[54] A. Dorigo,[54] F. Galeazzi,[54] M. Margoni,[54] M. Morandin,[54] M. Posocco,[54] M. Rotondo,[54] F. Simonetto,[54] R. Stroili,[54] G. Tiozzo,[54] C. Voci,[54] M. Benayoun,[55] H. Briand,[55] J. Chauveau,[55] P. David,[55] Ch. de la Vaissière,[55] L. Del Buono,[55] O. Hamon,[55] M. J. J. John,[55] Ph. Leruste,[55] J. Ocariz,[55] M. Pivk,[55] L. Roos,[55] J. Stark,[55] S. T'Jampens,[55] G. Therin,[55] P. F. Manfredi,[56] V. Re,[56] P. K. Behera,[57] L. Gladney,[57] Q. H. Guo,[57] J. Panetta,[57] C. Angelini,[58] G. Batignani,[58] S. Bettarini,[58] M. Bondioli,[58] F. Bucci,[58] G. Calderini,[58] M. Carpinelli,[58] V. Del Gamba,[58] F. Forti,[58] M. A. Giorgi,[58] A. Lusiani,[58] G. Marchiori,[58] F. Martinez-Vidal,[58, ‡] M. Morganti,[58] N. Neri,[58] E. Paoloni,[58] M. Rama,[58] G. Rizzo,[58] F. Sandrelli,[58] J. Walsh,[58] M. Haire,[59] D. Judd,[59] K. Paick,[59] D. E. Wagoner,[59] N. Danielson,[60] P. Elmer,[60] C. Lu,[60] V. Miftakov,[60] J. Olsen,[60] A. J. S. Smith,[60] H. A. Tanaka,[60] E. W. Varnes,[60] F. Bellini,[61] G. Cavoto,[60, 61] R. Faccini,[15, 61] F. Ferrarotto,[61] F. Ferroni,[61] M. Gaspero,[61] M. A. Mazzoni,[61] S. Morganti,[61] M. Pierini,[61] G. Piredda,[61] F. Safai Tehrani,[61] C. Voena,[61] S. Christ,[62] G. Wagner,[62] R. Waldi,[62] T. Adye,[63] N. De Groot,[63] B. Franek,[63] N. I. Geddes,[63] G. P. Gopal,[63] E. O. Olaiya,[63] S. M. Xella,[63] R. Aleksan,[64] S. Emery,[64] A. Gaidot,[64] S. F. Ganzhur,[64] P.-F. Giraud,[64] G. Hamel de Monchenault,[64] W. Kozanecki,[64] M. Langer,[64] M. Legendre,[64] G. W. London,[64] B. Mayer,[64] G. Schott,[64] G. Vasseur,[64] Ch. Yeche,[64] M. Zito,[64] M. V. Purohit,[65] A. W. Weidemann,[65] F. X. Yumiceva,[65] D. Aston,[66] R. Bartoldus,[66] N. Berger,[66] A. M. Boyarski,[66] O. L. Buchmueller,[66] M. R. Convery,[66] D. P. Coupal,[66] D. Dong,[66] J. Dorfan,[66] D. Dujmic,[66] W. Dunwoodie,[66] R. C. Field,[66] T. Glanzman,[66] S. J. Gowdy,[66] E. Grauges-Pous,[66] T. Hadig,[66] V. Halyo,[66] T. Hryn'ova,[66] W. R. Innes,[66] C. P. Jessop,[66] M. H. Kelsey,[66] P. Kim,[66] M. L. Kocian,[66] U. Langenegger,[66] D. W. G. S. Leith,[66] S. Luitz,[66] V. Luth,[66] H. L. Lynch,[66] H. Marsiske,[66] R. Messner,[66] D. R. Muller,[66] C. P. O'Grady,[66] V. E. Ozcan,[66] A. Perazzo,[66] M. Perl,[66] S. Petrak,[66] B. N. Ratcliff,[66] S. H. Robertson,[66] A. Roodman,[66] A. A. Salnikov,[66] R. H. Schindler,[66] J. Schwiening,[66] G. Simi,[66] A. Snyder,[66] A. Soha,[66] J. Stelzer,[66] D. Su,[66] M. K. Sullivan,[66] J. Va'vra,[66] S. R. Wagner,[66] M. Weaver,[66] A. J. R. Weinstein,[66] W. J. Wisniewski,[66] D. H. Wright,[66] C. C. Young,[66] P. R. Burchat,[67] A. J. Edwards,[67] T. I. Meyer,[67] B. A. Petersen,[67] C. Roat,[67] S. Ahmed,[68] M. S. Alam,[68] J. A. Ernst,[68] M. Saleem,[68] F. R. Wappler,[68] W. Bugg,[69] M. Krishnamurthy,[69] S. M. Spanier,[69] R. Eckmann,[70] H. Kim,[70] J. L. Ritchie,[70] R. F. Schwitters,[70] J. M. Izen,[71] I. Kitayama,[71] X. C. Lou,[71] S. Ye,[71] F. Bianchi,[72] M. Bona,[72] F. Gallo,[72] D. Gamba,[72] C. Borean,[73] L. Bosisio,[73] G. Della Ricca,[73] S. Dittongo,[73] S. Grancagnolo,[73] L. Lanceri,[73] P. Poropat,[73, §] L. Vitale,[73] G. Vuagnin,[73] R. S. Panvini,[74] Sw. Banerjee,[75] C. M. Brown,[75] D. Fortin,[75] P. D. Jackson,[75] R. Kowalewski,[75] J. M. Roney,[75] H. R. Band,[76] S. Dasu,[76] M. Datta,[76] A. M. Eichenbaum,[76] J. R. Johnson,[76] P. E. Kutter,[76] H. Li,[76] R. Liu,[76] F. Di Lodovico,[76] A. Mihalyi,[76] A. K. Mohapatra,[76] Y. Pan,[76] R. Prepost,[76] S. J. Sekula,[76] J. H. von Wimmersperg-Toeller,[76] J. Wu,[76] S. L. Wu,[76] Z. Yu,[76] and H. Neal[77]

(The *BABAR* Collaboration)

[1] *Laboratoire de Physique des Particules, F-74941 Annecy-le-Vieux, France*
[2] *Università di Bari, Dipartimento di Fisica and INFN, I-70126 Bari, Italy*
[3] *Institute of High Energy Physics, Beijing 100039, China*
[4] *University of Bergen, Inst. of Physics, N-5007 Bergen, Norway*
[5] *Lawrence Berkeley National Laboratory and University of California, Berkeley, CA 94720, USA*
[6] *University of Birmingham, Birmingham, B15 2TT, United Kingdom*
[7] *Ruhr Universität Bochum, Institut für Experimentalphysik 1, D-44780 Bochum, Germany*
[8] *University of Bristol, Bristol BS8 1TL, United Kingdom*
[9] *University of British Columbia, Vancouver, BC, Canada V6T 1Z1*
[10] *Brunel University, Uxbridge, Middlesex UB8 3PH, United Kingdom*
[11] *Budker Institute of Nuclear Physics, Novosibirsk 630090, Russia*
[12] *University of California at Irvine, Irvine, CA 92697, USA*
[13] *University of California at Los Angeles, Los Angeles, CA 90024, USA*
[14] *University of California at Riverside, Riverside, CA 92521, USA*
[15] *University of California at San Diego, La Jolla, CA 92093, USA*
[16] *University of California at Santa Barbara, Santa Barbara, CA 93106, USA*
[17] *University of California at Santa Cruz, Institute for Particle Physics, Santa Cruz, CA 95064, USA*
[18] *California Institute of Technology, Pasadena, CA 91125, USA*
[19] *University of Cincinnati, Cincinnati, OH 45221, USA*

[20]*University of Colorado, Boulder, CO 80309, USA*
[21]*Colorado State University, Fort Collins, CO 80523, USA*
[22]*Technische Universität Dresden, Institut für Kern- und Teilchenphysik, D-01062 Dresden, Germany*
[23]*Ecole Polytechnique, LLR, F-91128 Palaiseau, France*
[24]*University of Edinburgh, Edinburgh EH9 3JZ, United Kingdom*
[25]*Università di Ferrara, Dipartimento di Fisica and INFN, I-44100 Ferrara, Italy*
[26]*Florida A&M University, Tallahassee, FL 32307, USA*
[27]*Laboratori Nazionali di Frascati dell'INFN, I-00044 Frascati, Italy*
[28]*Università di Genova, Dipartimento di Fisica and INFN, I-16146 Genova, Italy*
[29]*Harvard University, Cambridge, MA 02138, USA*
[30]*Imperial College London, London, SW7 2BW, United Kingdom*
[31]*University of Iowa, Iowa City, IA 52242, USA*
[32]*Iowa State University, Ames, IA 50011-3160, USA*
[33]*Laboratoire de l'Accélérateur Linéaire, F-91898 Orsay, France*
[34]*Lawrence Livermore National Laboratory, Livermore, CA 94550, USA*
[35]*University of Liverpool, Liverpool L69 3BX, United Kingdom*
[36]*Queen Mary, University of London, E1 4NS, United Kingdom*
[37]*University of London, Royal Holloway and Bedford New College, Egham, Surrey TW20 0EX, United Kingdom*
[38]*University of Louisville, Louisville, KY 40292, USA*
[39]*University of Manchester, Manchester M13 9PL, United Kingdom*
[40]*University of Maryland, College Park, MD 20742, USA*
[41]*University of Massachusetts, Amherst, MA 01003, USA*
[42]*Massachusetts Institute of Technology, Laboratory for Nuclear Science, Cambridge, MA 02139, USA*
[43]*McGill University, Montréal, QC, Canada H3A 2T8*
[44]*Università di Milano, Dipartimento di Fisica and INFN, I-20133 Milano, Italy*
[45]*University of Mississippi, University, MS 38677, USA*
[46]*Université de Montréal, Laboratoire René J. A. Lévesque, Montréal, QC, Canada H3C 3J7*
[47]*Mount Holyoke College, South Hadley, MA 01075, USA*
[48]*Università di Napoli Federico II, Dipartimento di Scienze Fisiche and INFN, I-80126, Napoli, Italy*
[49]*NIKHEF, National Institute for Nuclear Physics and High Energy Physics, NL-1009 DB Amsterdam, The Netherlands*
[50]*University of Notre Dame, Notre Dame, IN 46556, USA*
[51]*Oak Ridge National Laboratory, Oak Ridge, TN 37831, USA*
[52]*Ohio State University, Columbus, OH 43210, USA*
[53]*University of Oregon, Eugene, OR 97403, USA*
[54]*Università di Padova, Dipartimento di Fisica and INFN, I-35131 Padova, Italy*
[55]*Universités Paris VI et VII, Lab de Physique Nucléaire H. E., F-75252 Paris, France*
[56]*Università di Pavia, Dipartimento di Elettronica and INFN, I-27100 Pavia, Italy*
[57]*University of Pennsylvania, Philadelphia, PA 19104, USA*
[58]*Università di Pisa, Dipartimento di Fisica, Scuola Normale Superiore and INFN, I-56127 Pisa, Italy*
[59]*Prairie View A&M University, Prairie View, TX 77446, USA*
[60]*Princeton University, Princeton, NJ 08544, USA*
[61]*Università di Roma La Sapienza, Dipartimento di Fisica and INFN, I-00185 Roma, Italy*
[62]*Universität Rostock, D-18051 Rostock, Germany*
[63]*Rutherford Appleton Laboratory, Chilton, Didcot, Oxon, OX11 0QX, United Kingdom*
[64]*DSM/Dapnia, CEA/Saclay, F-91191 Gif-sur-Yvette, France*
[65]*University of South Carolina, Columbia, SC 29208, USA*
[66]*Stanford Linear Accelerator Center, Stanford, CA 94309, USA*
[67]*Stanford University, Stanford, CA 94305-4060, USA*
[68]*State Univ. of New York, Albany, NY 12222, USA*
[69]*University of Tennessee, Knoxville, TN 37996, USA*
[70]*University of Texas at Austin, Austin, TX 78712, USA*
[71]*University of Texas at Dallas, Richardson, TX 75083, USA*
[72]*Università di Torino, Dipartimento di Fisica Sperimentale and INFN, I-10125 Torino, Italy*
[73]*Università di Trieste, Dipartimento di Fisica and INFN, I-34127 Trieste, Italy*
[74]*Vanderbilt University, Nashville, TN 37235, USA*
[75]*University of Victoria, Victoria, BC, Canada V8W 3P6*
[76]*University of Wisconsin, Madison, WI 53706, USA*
[77]*Yale University, New Haven, CT 06511, USA*

(Dated: January 10, 2018)

We present results of searches for B-meson decays to $K^+\pi^-\pi^+$ with the *BABAR* detector. With a data sample of 61.6 million $B\overline{B}$ pairs, we measure the branching fractions and 90% confidence-level upper limits averaged over charge-conjugate states (the first error is statistical and the second is systematic): $\mathcal{B}(B^+ \to K^{*0}(892)\pi^+) = (15.5 \pm 1.8^{+1.5}_{-4.0}) \times 10^{-6}$, $\mathcal{B}(B^+ \to f_0(980)K^+, f_0 \to$

$\pi^+\pi^-) = (9.2 \pm 1.2^{+2.1}_{-2.6}) \times 10^{-6}$, $\mathcal{B}(B^+ \to \overline{D}^0\pi^+, \overline{D}^0 \to K^+\pi^-) = (184.6 \pm 3.2 \pm 9.7) \times 10^{-6}$, $\mathcal{B}(B^+ \to \rho^0(770)K^+) < 6.2 \times 10^{-6}$ and $\mathcal{B}(B^+ \to K^+\pi^-\pi^+$ non-resonant$) < 17 \times 10^{-6}$.

PACS numbers: 13.25.Hw, 12.15.Hh, 11.30.Er

The study of charmless hadronic B decays can make important contributions to our understanding of hadronic decays and *CP* violation in the Standard Model [1]. Branching fraction predictions for B meson decays to Pseudoscalar–Vector final states have recently been calculated using QCD Factorisation and SU(3) flavor symmetry models [2, 3, 4]. The measurement of B^+ meson [5] decays to the final state $K^+\pi^-\pi^+$ via intermediate resonances can be used to search for weak phases and direct *CP* violation. The signal can be used to examine the light-meson mass spectrum [6, 7]. The charm state χ_{c0} might be sensitive to the angle γ of the Unitarity Triangle through interference with the non-resonant component producing an observable charge asymmetry [8]; the branching fraction also constrains some models for charmonium hybrid production [9].

The data used in this analysis were collected at the PEP-II asymmetric e^+e^- storage ring with the *BABAR* detector [10]. The *BABAR* detector consists of a five-layer silicon tracker, a drift chamber, a new type of Cherenkov detector [11], an electromagnetic calorimeter and a magnet with instrumented flux return. The data sample has an integrated luminosity of 56.4 fb^{-1} collected at the $\Upsilon(4S)$ resonance, which corresponds to $(61.6 \pm 0.7) \times 10^6$ $B\overline{B}$ pairs ($N_{B\overline{B}}$). We assume that the $\Upsilon(4S)$ decays equally to neutral and charged B meson pairs.

The $K^+\pi^-\pi^+$ phase space can be represented in a Dalitz plot, in which the many resonant B decay modes form overlapping bands and interference occurs where the bands overlap [12]. As a consequence, the whole Dalitz plot should be considered before assigning a branching fraction to a specific mode. However, the data sample is not large enough for a full Dalitz plot fit to be effective. In this analysis, the Dalitz plot is divided into eight regions, reflecting as much as possible the known decay modes. We first determine the yields in these regions using a maximum-likelihood fit. We then interpret the yields as branching fractions, assuming a particular collection of quasi-two-body decay modes. We evaluate the systematic uncertainty due to the particular choice of decay modes and the effect of interference between the different contributions.

The regions are defined in $m_{K\pi}$ and $m_{\pi\pi}$, the invariant masses of the neutral $K\pi$ and $\pi\pi$ systems, as given in Table I and illustrated in Fig. 1. Region I is expected to be dominated by $K^{*0}(892)\pi^+$. Region II could have contributions from several higher K^* resonances. Region III is dominated by the production of $\overline{D}^0\pi^+$. The high branching fraction for this mode allows it to be used to correct for differences between data and simulated events and to evaluate systematic uncertainties. Regions IV and V are expected to be dominated by $\rho^0(770)K^+$ and $f_0(980)K^+$, respectively. The resonance contributions to Region VI are not known a priori. The area where these regions intersect the $\overline{D}^0$ band, $1.8 < m_{K\pi} < 1.9\,\mathrm{GeV}/c^2$, is excluded. Region VII could contain higher mass charmless and charmonium resonances, as well as a non-resonant contribution that extends across the whole Dalitz plot. Region VIII is dominated by $\chi_{c0}K^+$. This channel is vetoed from other regions using $3.355 < m_{\pi\pi} < 3.475\,\mathrm{GeV}/c^2$.

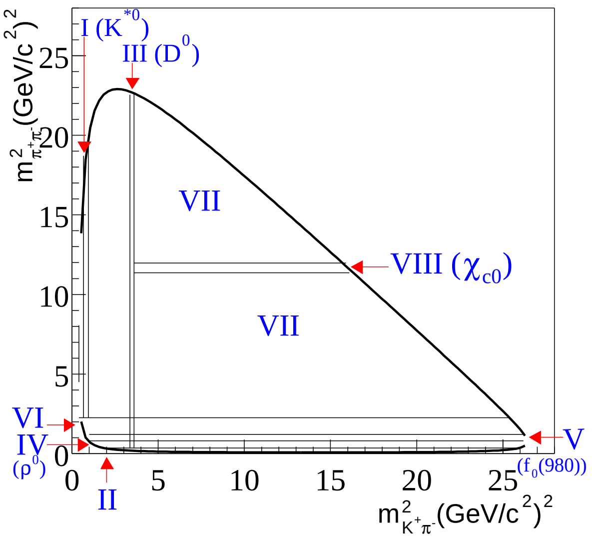

FIG. 1: A Dalitz plot showing the defined regions.

TABLE I: Regions of the $K^+\pi^-\pi^+$ Dalitz plot and signal yields obtained (the first error is statistical and the second is systematic). The $\overline{D}^0$ band, $1.8 < m_{K\pi} < 1.9\,\mathrm{GeV}/c^2$, is excluded from all regions except region III, and the χ_{c0} band, $3.355 < m_{\pi\pi} < 3.475\,\mathrm{GeV}/c^2$, is excluded from all regions except region VIII.

Region	Selection Criteria (GeV/c^2)	Signal Yield
I	$0.816 < m_{K\pi} < 0.976$, $m_{\pi\pi} > 1.5$	$161 \pm 18 \pm 4$
II	$0.976 < m_{K\pi} < 1.8$, $m_{\pi\pi} > 1.5$	$405 \pm 28 \pm 13$
III	$1.835 < m_{K\pi} < 1.895$	$3755 \pm 66 \pm 11$
IV	$0.6 < m_{\pi\pi} < 0.9$	$66 \pm 15^{+3}_{-7}$
V	$0.9 < m_{\pi\pi} < 1.1$	$179 \pm 19 \pm 5$
VI	$1.1 < m_{\pi\pi} < 1.5$	$126 \pm 19 \pm 5$
VII	$m_{K\pi} > 1.9$, $m_{\pi\pi} > 1.5$	$133 \pm 23^{+9}_{-22}$
VIII	$m_{K\pi} > 1.9$, $3.37 < m_{\pi\pi} < 3.46$	$26 \pm 6 \pm 1$

Candidate B mesons are formed by combining three charged tracks, where each track is required to have at least 12 hits in the drift chamber, to have transverse momentum of at least 100 MeV/c and to be consistent with originating from the beam-spot. Charged pions and kaons are identified using energy loss ($\mathrm{d}E/\mathrm{d}x$) measured in the tracking system and the Cherenkov angle and number of photons measured by the Cherenkov detector. Pions are required to fail the kaon selection. The efficiency of selecting kaons is approximately 80%, while the probability of misidentifying pions as kaons is below 5%, up to a laboratory momentum of 4.0 GeV/c. Pions are also required to fail an electron selector which uses $\mathrm{d}E/\mathrm{d}x$, the energy to momentum ratio and the shape of the calorimeter signal. Over 99% of pions from the signal decay pass this requirement.

Signal decays are identified using two kinematic variables: ΔE, the difference between the center-of-mass (CM) energy of the B candidate and $\sqrt{s}/2$, where $\sqrt{s}$ is the total CM energy; and the beam-energy-substituted mass $m_{\mathrm{ES}} = \sqrt{(s/2 + \mathbf{p}_i \cdot \mathbf{p}_B)^2/E_i^2 - \mathbf{p}_B^2}$, where $\mathbf{p}_B$ is the momentum of the reconstructed B candidate and $(E_i, \mathbf{p}_i)$ is the four-momentum of the initial e^+e^- system. The ΔE and m_{ES} distributions for signal events have widths of 20 MeV and 2.7 MeV/c^2, respectively. We require $5.22 < m_{\mathrm{ES}} < 5.29\,\mathrm{GeV}/c^2$ and $|\Delta E| < 0.1\,\mathrm{GeV}$ for events entering the fit. Events with $0.1 < |\Delta E| < 0.3\,\mathrm{GeV}$ are used for continuum background characterisation as described below.

A very small proportion of events, fewer than 4%, have two or more candidates that pass the above requirements. For these events a single candidate is selected at random, so as not to bias the fit distributions. This random selection has a minimal impact on the efficiency, and any systematic uncertainty due to this effect is negligible. A single candidate per event is similarly selected for the data with $0.1 < |\Delta E| < 0.3\,\mathrm{GeV}$ used in continuum background characterisation.

Continuum light-quark and charm production is the dominant source of background. This is suppressed using two event-shape variables. The first is the cosine of the angle θ_T between the thrust axis of the selected B candidate and the thrust axis of the rest of the event. For continuum background, the distribution of $|\cos\theta_T|$ is strongly peaked towards unity whereas the distribution is uniform for signal events. We require $|\cos\theta_T| < 0.9$. The second event-shape variable is a Fisher discriminant ($\mathcal{F}$) [13]. For $\mathcal{F}$ we use a linear combination of the cosine of the angle between the B-candidate momentum and the beam axis, the cosine of the angle between the B-candidate thrust axis and the beam axis, and the energy flow of the rest of the event into each of nine contiguous, concentric, 10° cones around the thrust axis of the reconstructed B [14].

There are also B-decay backgrounds, mainly four-body decays, and three-body decays with one or more particles misidentified. These backgrounds are studied using Monte Carlo simulations (MC). They are reduced by the particle identification selections and by excluding events containing J/ψ or $\psi(2S)$ decays to l^+l^- with vetoes $2.97 < m_{\pi\pi} < 3.17\,\mathrm{GeV}/c^2$ and $3.56 < m_{\pi\pi} < 3.76\,\mathrm{GeV}/c^2$, however some B-decay backgrounds remain and must be accounted for. For backgrounds contributing only a few events to the maximum-likelihood (ML) fit, the estimated contribution is subtracted from the final signal yield with a systematic uncertainty to account for the unknown probability of the background to be selected as signal in the fit. Larger backgrounds are parameterized in the ML fit as described below. These were $B^+ \to \overline{D}{}^0\pi^+, \overline{D}{}^0 \to K^+\pi^-\pi^0$ in regions II and VII, $B^+ \to \overline{D}{}^0\rho^+(770)$ with $\overline{D}{}^0 \to K^+\pi^-$ and $\rho^+ \to \pi^+\pi^0$ in region VII and $B^+ \to \eta' K^+$ with $\eta' \to \rho^0(770)\gamma$, $\rho^0 \to \pi^+\pi^-$ in regions IV and V.

We form probability density functions (PDFs) with parameters $\vec{\alpha}$ for the three variables ($\vec{x}$) m_{ES}, ΔE, and $\mathcal{F}$ in each region. We find the correlations among these variables to be negligible; accordingly, for each hypothesis l (signal, continuum background, and B background), we form a product $P_l = P_{l,m_{\mathrm{ES}}} P_{l,\Delta E} P_{l,\mathcal{F}}$ that models that hypothesis. The likelihood for an event j is the sum over the M hypotheses of the products P_l, with each product weighted by the number of events (to be determined), n_l, for that hypothesis. A product over the N events in the data sample of the event likelihoods along with a Poisson factor forms the likelihood function:

$$\mathcal{L} = \exp\left(-\sum_{i=1}^{M} n_i\right) \prod_{j=1}^{N} \left(\sum_{l=1}^{M} n_l\, P_l(\vec{\alpha}, \vec{x_j})\right). \qquad (1)$$

This likelihood is maximized to obtain n_l for the signal and continuum background components; n_l for the B-background component is fixed to an estimate of the contribution from MC. The parameters of the signal and B-background PDFs are determined from MC and held fixed in the final fit. The continuum background parameters for $\mathcal{F}$ are fixed from the data with $0.1 < |\Delta E| < 0.3\,\mathrm{GeV}$. The continuum background parameters for ΔE and m_{ES} are left free in the final fit. Each m_{ES} PDF is a Gaussian distribution for signal, and an ARGUS threshold function [15] for continuum background. Each ΔE PDF is a sum of two Gaussian distributions with equal means for the signal and a first-degree polynomial for the continuum background. The signal and background $\mathcal{F}$ PDFs are Gaussian distributions with different widths above and below the mean. For the B-background parameterizations, signal or continuum shapes are used depending on the nature of the background. The projections of the Region I data in m_{ES}, ΔE and $\mathcal{F}$ and the results of the fit are shown in Fig. 2, demonstrating a clear signal. The data in the plots pass a selection on the per-event signal-to-background likelihood ratio formed from the other two fit variables, which has been optimized to give the greatest significance to the signal.

The signal yields for the regions of the Dalitz plot

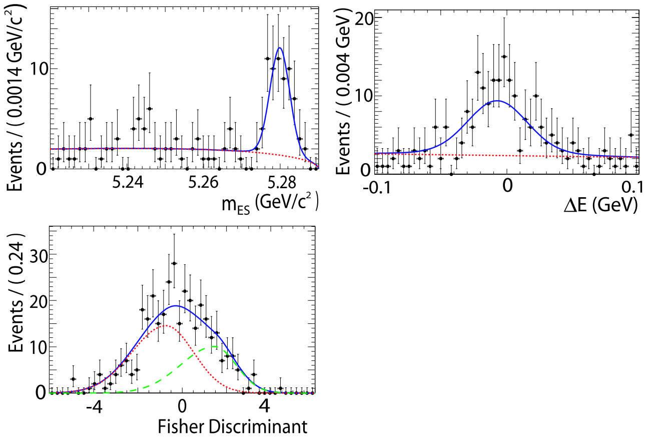

FIG. 2: Projection plots in m_{ES}, ΔE and $\mathcal{F}$, for the data in Region I. The superimposed curve is a projection of the full fit with the background component shown as a dotted line and, for $\mathcal{F}$, the signal component shown as a dashed line.

TABLE II: A summary of the model used to calculate branching fractions. Alternative lineshapes are given in parentheses. The masses and widths are taken from the Review of Particle Physics [6].

Resonance	Lineshape	Mass (MeV/c^2)	Width (MeV/c^2)
$K^{*0}(892)$	BW	896.10 ± 0.27	50.7 ± 0.6
$K_0^{*0}(1430)$	BW (LASS[16])	1412 ± 6	294 ± 23
D^0	BW	1864.5 ± 0.5	0
$\rho^0(770)$	Blatt-Weisskopf[17]	769.0 ± 0.9	150.9 ± 1.7
$f_0(980)$	BW (Flatté[18])	980 ± 10	70 ± 30
$f_2(1270)$	BW	1275 ± 12	185 ± 30
χ_{c0}	BW	3415.1 ± 0.8	16.2 ± 3.2
non-resonant	flat	all masses	-

are shown in Table I. The systematic uncertainty arises from the PDF parameters and from B-background subtraction. We find that all yields have a significance greater than five standard deviations, where $\sqrt{2\ln(\mathcal{L}_{max}/\mathcal{L}_{max(n_{signal}=0)})}$ is used as an estimator of the significance.

We calculate the branching fractions from the measured yields, taking into account the overlapping nature of the resonances, using $\mathcal{B} = \mathrm{M}^{-1}\ \mathrm{Y}/N_{B\overline{B}}$ where Y is a vector of the yields in each Dalitz region and $\mathcal{B}$ is a vector of branching fractions. M is the efficiency matrix where M_{ij} is the probability that an event arising from the contribution dominating region i will be found in region j. The elements of M are estimated using MC including small corrections for differences in tracking and in particle identification efficiencies between MC and data, and differences between MC and our resonance model.

In our resonance model we assume one dominant contribution per region. The contributions for the chosen model are given in Table II. For Regions II and VI where the main contributions are not known a priori, we take the dominant contributions to be $K_0^{*0}(1430)\pi^+$ and $f_2(1270)K^+$ respectively. However, we quote branching fractions for $B^+ \to$"higher K^{*0}"π^+ where "higher K^{*0}" means any combination of $K_0^{*0}(1430), K_2^{*0}(1430)$ and $K_1^{*0}(1680)$ and $B^+ \to$"higher f"K^+, where "higher f" means any combination of $f_2(1270)$, $f_0(1370)$ and $f_2(1430)$. Non-relativistic Breit–Wigner line shapes are used for all channels except for the broad $\rho(770)$ resonance, where we use a relativistic Breit–Wigner line shape with Blatt–Weisskopf damping [17].

TABLE III: The measured branching fractions and uncertainties. The first uncertainty is statistical, the second includes the systematic uncertainties from the yields and the efficiencies, the third is the model uncertainty, and the fourth is the uncertainty due to interference.

Channel	BF $\times 10^{-6}$
$K^{*0}(892)\pi^+$	$15.5 \pm 1.8 \pm 1.1^{+0.6}_{-3.8} \pm 0.9$
"higher K^{*0}"π^+, $K^{*0} \to K^+\pi^-$	$25.1 \pm 2.0 \pm 2.9^{+9.4}_{-0.5} \pm 4.9$
$\overline{D}^0\ \pi^+$, $\overline{D}^0 \to K^+\pi^-$	$184.6 \pm 3.2 \pm 9.7$
$\rho^0(770)K^+$	$3.9 \pm 1.2^{+0.3+0.3}_{-0.6-3.2} \pm 1.2$
$f_0(980)K^+$, $f_0 \to \pi^+\pi^-$	$9.2 \pm 1.2 \pm 0.6^{+1.2}_{-1.9} \pm 1.6$
"higher f"K^+, $f \to \pi^+\pi^-$	$3.2 \pm 1.2 \pm 0.5^{+5.8}_{-2.4} \pm 1.5$
Non-resonant	$5.2 \pm 1.9^{+0.8+3.3}_{-1.8-7.5} \pm 6.4$
$\chi_{c0}K^+$, $\chi_{c0} \to \pi^+\pi^-$	$1.5 \pm 0.4 \pm 0.1$

We evaluate systematic uncertainties on the branching fractions taking into consideration uncertainties on resonance parameters and alternative line shapes given in Table II. We also include the effect on all branching fractions that in Regions II and VI, the dominant contribution could be any combination of a number of resonances. Also included in the systematic uncertainties is the possibility that the yield measured in Region VII is from a resonant component and does not extend into the other regions. Uncertainties on the branching fractions due to the interference between the resonances are evaluated by generating many simulated $B^+ \to K^+\pi^-\pi^+$ Dalitz plots with all the contributions having random phases and observing how the interference between the contributions affects the measured branching fractions. The branching fractions and uncertainties of intermediate resonances are given in Table III.

Fig. 3 shows the Dalitz plot for data events within a signal region, $5.2715 < m_{\rm ES} < 5.2865\,{\rm GeV}/c^2$, that have a the per-event signal-to-background likelihood ratio formed from the ΔE and $\mathcal{F}$ PDFs, greater than 5. Both signal and background events appear in the plot. The $\overline{D}^0\ \pi^+$ signal is the narrow band in the $m_{K\pi}$ spectrum. To illustrate the expected background distribution, events passing the same likelihood selection but having a value of $m_{\rm ES}$ between $5.25 < m_{\rm ES} < 5.26\,{\rm GeV}/c^2$ are also shown. The size of this sideband is chosen to contain approximately the expected number of background

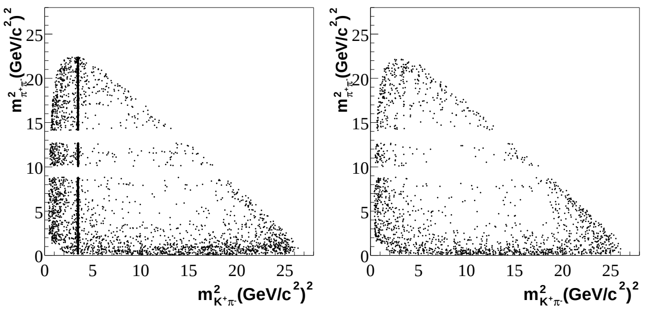

FIG. 3: Dalitz plots showing (left) the observed distribution in a signal $m_{\rm ES}$ region (defined in the text) and (right) the distribution for continuum background from the $m_{\rm ES}$ sideband. Vetoes reject events with J/ψ and $\psi(2S)$.

events that will enter the signal-region plot.

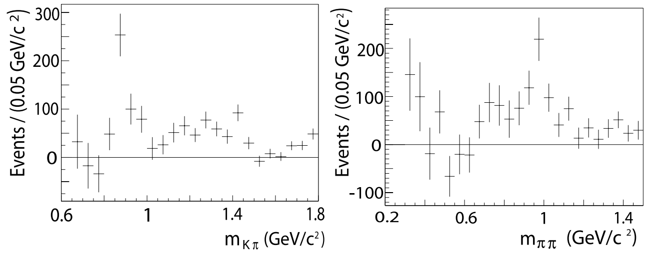

FIG. 4: Background-subtracted and efficiency-corrected projections of the Dalitz plot in $m_{K\pi}$ and $m_{\pi\pi}$.

Fig. 4 shows background-subtracted, efficiency–corrected projections of the two-body invariant mass spectra, $m_{K\pi}$ and $m_{\pi\pi}$, from $0.6\,{\rm GeV}/c^2$ to $1.8\,{\rm GeV}/c^2$ and from $0.2\,{\rm GeV}/c^2$ to $1.5\,{\rm GeV}/c^2$ respectively. The signal events and background distributions are obtained by the same method as for Fig. 3 and again the $\overline{D}^0$, J/Ψ and $\Psi(2S)$ vetoes are applied. Peaks at the $K^{*0}(892)$ and $f_0(980)$ masses are clearly visible.

The invariant mass $m_{K\pi}$ or $m_{\pi\pi}$, and helicity angle between the resonance decay and flight directions, θ_H, are not used in the likelihood fit. However, to illustrate our findings, we show, in Fig. 5, resonant mass and $\cos\theta_H$ projections for Regions I, IV and II after background subtraction and efficiency corrections. Figs. 5(a–d) have been overlaid with the distribution of the expected dominant resonance: Breit–Wigner line shapes for the mass distributions in Figs. 5(a) and 5(c), $\cos^2\theta_H$ for the $K^{*0}(892)$ $\cos\theta_H$ distribution in Fig. 5(b), and a uniform distribution for the scalar $f_0(980)$ $\cos\theta_H$ distribution in Fig. 5(d). There is good agreement between the overlaid and observed distributions indicating that the expected resonances are indeed dominant in these regions. The $f_0(980)$ $\cos\theta_H$ distribution suggests a linear dependence that is most likely due to interference with the vector $\rho(770)$, which is taken into account in our interference systematic uncertainty.

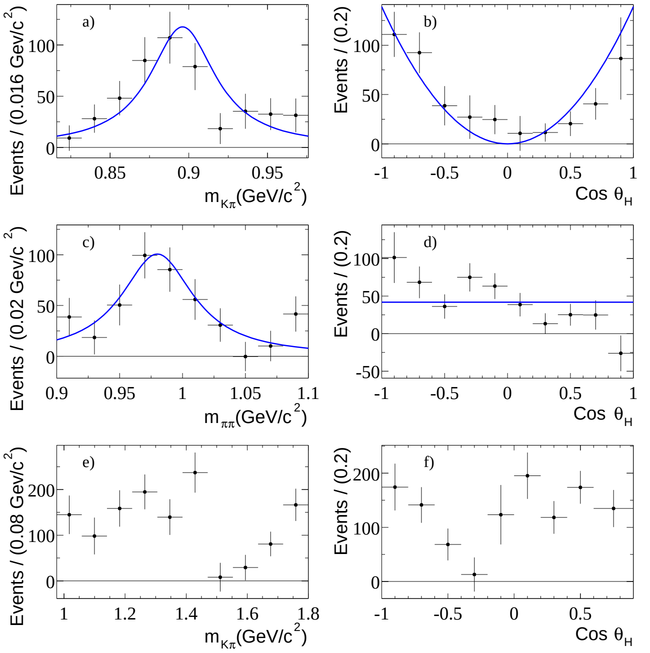

FIG. 5: Projection plots of the two-body invariant mass and $\cos\theta_H$ for, from top to bottom, Regions I, V and II.

We can see in Fig 4, there is a large signal in the region $1.1 < m_{K\pi} < 1.4\,{\rm GeV}/c^2$ (Region II). This is shown in more detail in Fig. 5(e), resonant mass, and Fig. 5(f), the $\cos\theta_H$ projections for Region II. The complex behavior of this signal is similar to that observed by LASS [16] and precludes an interpretation as a single resonance.

In conclusion, we have made branching fraction measurements, summarized in Table III, for a number of charm and charmless B decay channels with the final state $K^+\pi^-\pi^+$. This analysis has taken into account the uncertainty in the knowledge of the nature and parameterization of the intermediate resonances on all the branching fractions assuming a non-resonant contribution with kinematics defined by phase space. The results also take account of the unknown levels of interference between the different contributions. The $B^+ \to \overline{D}^0\pi^+$ and $B^+ \to \chi_{c0}K^+$ results agree with previous measurements [19, 20]. The $B^+ \to K^{*0}(892)\pi^+$ [21] and $B^+ \to f_0(980)K^+$ branching fractions are consistent with, and more precise than, previous measurements [22]. The $B^+ \to K^{*0}(892)\pi^+$ result is significantly higher than predicted by many factorization models [3]. The observation of the decay $B^+ \to f_0(980)K^+$ provides hints about the nature of the $f_0(980)$ [7]. A large signal is seen for $B^+ \to$"higher K^{*0}"π^+ where "higher K^{*0}" means any combination of $K_0^{*0}(1430)$, $K_2^{*0}(1430)$ and $K_1^{*0}(1680)$.

We also give 90% confidence-level upper limits for the branching fractions of the following channels: $\mathcal{B}(B^+ \to \rho^0(770)K^+) < 6.2\times10^{-6}$, $\mathcal{B}(B^+ \to K^+\pi^-\pi^+$ non-resonant$) < 17\times10^{-6}$, $\mathcal{B}(B^+ \to$"higher f"$K^+) < 12\times10^{-6}$. The tight limit on the non-resonant component means that its γ-dependent interference with the $\chi_{c0}K$ final state will be very hard to measure.

We are grateful for the excellent luminosity and machine conditions provided by our PEP-II colleagues, and for the substantial dedicated effort from the computing organizations that support *BABAR*. The collaborating institutions wish to thank SLAC for its support and kind hospitality. This work is supported by DOE and NSF (USA), NSERC (Canada), IHEP (China), CEA and CNRS-IN2P3 (France), BMBF and DFG (Germany), INFN (Italy), FOM (The Netherlands), NFR (Norway), MIST (Russia), and PPARC (United Kingdom). Individuals have received support from CONACyT (Mexico), A. P. Sloan Foundation, Research Corporation, and Alexander von Humboldt Foundation.

---

[*] Also with Università di Perugia, Perugia, Italy

[†] Also with Università della Basilicata, Potenza, Italy

[‡] Also with IFIC, Instituto de Física Corpuscular, CSIC-Universidad de Valencia, Valencia, Spain

[§] Deceased

[1] M. Beneke, *et al.*, Nucl. Phys. B **591**, 313 (2000).

[2] M. Beneke and M. Neubert, Nucl. Phys. B **675**, 333 (2003).

[3] W. N. Cottingham, *et al.*, J. Phys. G **28**, 2843 (2002).

[4] Cheng-Wei Chiang, *et al.*, Phys. Rev. D **69**, 034001 (2004).

[5] Throughout this paper, flavor-eigenstate decay modes imply also their charge conjugate.

[6] Particle Data Group, K. Hagiwara, *et al.*, Phys. Rev. D **66**, 010001 (2002).

[7] P. Minkowski and W. Ochs, hep-ph/0304144.

[8] S. Fajfer, R. J. Oakes and T. N. Pham, Phys. Lett. B **539**, 67 (2002).

[9] F. E. Close and S. Godfrey Phys. Lett. B **574**, 210 (2003).

[10] *BABAR* Collaboration, B. Aubert, *et al.*, Nucl. Instr. Meth. A **479**, 1 (2002).

[11] J. Schwiening, *et al.*, NIM A **502**, 67-75 (2003).

[12] R. H. Dalitz, Phil. Mag. **44**, 1068 (1953).

[13] R. A. Fisher, Ann. Eugenics **7**, 179 (1936); G. Cowan, *Statistical Data Analysis*, 51 (Oxford University Press, 1998).

[14] CLEO Collaboration, D. M. Asner, *et al.*, Phys. Rev. D **53**, 1039 (1996).

[15] ARGUS Collaboration, H. Albrecht, *et al.*, Z. Phys. C **48**, 543 (1990).

[16] LASS Collaboration, D. Aston, *et al.*, Nucl. Phys. B **296**, 493 (1988).

[17] J. M. Blatt and V. F. Weisskopf, *Theoretical Nuclear Physics* 361 (Wiley, New York, 1952).

[18] S. M. Flatté, Phys. Lett. B **63**, 224 (1976).

[19] CLEO Collaboration, Phys. Rev. D **66**, 031101(R) (2002)

[20] Belle Collaboration, K. Abe, *et al.*, Phys. Rev. Lett. **88**, 031802 (2002)

[21] The comparison takes into account that the secondary branching fraction of $K^{*0} \to K^+\pi^-$ is 2/3.

[22] Belle Collaboration, K. Abe, *et al.*, Phys. Rev. D **65**, 092005 (2002).